GLYCOGEN DISTRIBUTION AND METABOLIC ALTERATIONS IN THE HYPERMUSCULAR, MYOSTATIN MUTANT *COMPACT* MICE

Summary of Ph.D. Thesis

Tamás Kocsis, MD

Supervisor: Anikó Keller-Pintér, MD, Ph.D.

Department of Biochemistry

Doctoral School of Multidisciplinary Medical Science

Faculty of Medicine

University of Szeged

Szeged

2017

PUBLICATIONS

1. Publications related to the subject of the dissertation:

Kocsis T, Baán J, Müller G, Mendler L, Dux L, Keller-Pintér A. Skeletal muscle celullarity and glycogen distribution in the hypermuscular *Compact* mice. *Eur J Histochem* 58: 2353, 2014. [IF: 2.042]

Kocsis T, Trencsenyi G, Szabo K, Baan JA, Muller G, Mendler L, Garai I, Reinauer H, Deak F, Dux L, Keller-Pinter A. Myostatin propeptide mutation of the hypermuscular *Compact* mice decreases the formation of myostatin and improves insulin sensitivity. *Am J Physiol Endocrinol Metab* 312(3):E150-E160, 2017. [IF: 4.142* (2016)]

2. Other full paper published during the Ph.D fellowship:

Baán JA, **Kocsis T,** Keller-Pintér A, Müller G, Zádor E, Dux L, Mendler L. The *Compact* mutation of myostatin causes a glycolytic shift in the phenotype of fast skeletal muscles. *J Histochem Cytochem* 12: 889-900, 2013. [IF: 2.412]

INTRODUCTION

Myostatin (Growth/Differentation Factor 8)

The TGF-β (Transforming Growth Factor-β) superfamily member myostatin is a potent regulator of the skeletal muscle mass. Knocking out of the myostatin gene leads to increased muscle mass with hyperplasia and hypertrophy of the muscle fibers. Furthermore, naturally occurring myostatin gene mutations, e.g., in humans, mouse, cattle, or sheep were described resulting in widespread increase of skeletal muscle mass ("double-muscled" phenotype). Myostatin regulates the proliferation and differentiation of myoblasts; moreover, it also controls the activation and proliferation of satellite cells, the stem cells of skeletal muscle.

Myostatin signaling and the regulation of skeletal muscle mass

TGF-superfamily members signal through heteromeric receptor complexes composed of two homodimers each of type I and type II serine/threonine kinase receptors. The activated anaplastic lymphoma kinase type I receptor (ALK4 or ALK5) then propagates the signal by phosphorylating Smad2/3 transcriptional factors. The phospho-Smad2/3 molecules forms an oligomer with Smad4 that translocates into the nucleus where it interacts with Smad binding partners to regulate transcription. Beyond the Smad2/3 mediated signaling, myostatin influences the phosphatidylinositol 3-kinase (PI3K)/Akt pathway, which is the key regulator of the anabolic and catabolic responses in skeletal muscle. Myostatin stimulates cyclin D1 degradation though a PI3K/Akt pathway leading to cell cycle arrest.

The role of myostatin in glucose metabolism

Myostatin-null mice exhibit increased muscle mass, reduced body fat, and increased insulin sensitivity, which depends on AMP-activated protein kinase. In accordance with increased insulin sensitivity, also detected elevated levels of GLUT4 (Glucose transporter type 4), pAkt and IRS-1 (Insulin Receptor Substrate-1) in *mstn* −/− muscles. Transgenic expression of myostatin propeptide prevents diet-induced obesity and insulin resistance, and the overexpression of follistatin-like 3, an inhibitor of members of the TGFβ family, or inhibition of myostatin by dominant-negative myostatin receptor also improves insulin

sensitivity. Myostatin was reported to influence the synthesis and secretion of IGF-1 (Insulin-like Growth Factor 1) in the liver, thereby regulating the amount of circulating IGF-1.

The *Compact* mutation and the *Compact* mice

The naturally occurring *Compact* mutation of the myostatin gene arose in a selection program on protein amount and hypermuscularity conducted at the Technical University of Berlin. Genetic analysis of the Hungarian subpopulation of the hypermuscular *Compact* mice identified a 12-bp deletion, denoted *Mstn(Cmpt-dl1Abc)*, in the propeptide of the promyostatin. This non-frameshift mutation leads to the shortening of the propeptide region. Both the furin cleavage site and the biologically active growth factor domain of myostatin are unaffected by the *Compact* mutation **(Figure 1)**. Therefore, the loss of myostatin activity cannot be explained by disruption of the growth factor bioactive domain; however, the mutation can lead to misfolding, or defect in secretion and mistargeting of mature myostatin.

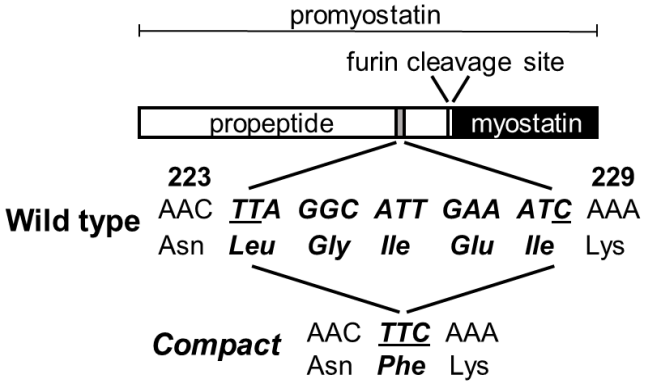

Figure 1. *Schematic representation of the non-frameshift Compact mutation in the propeptide region of promyostatin.*

Additional modifier genes should be present to determine the full expression of the *Compact* phenotype; however, these modifier genes of the special *Compact* genetic background have not yet been identified. Markers on several chromosomes (chromosomes 1, 3, 5, 7, 11, 16 and X) showed linkage with the putative modifiers, and the strongest association was found for markers on chromosomes 16 and X.

AIMS

Although the *Compact* mutation was identified in 1998, its precise molecular effects have not yet been examined. In this study, by using a congenic wild-type mice strain with wild-type myostatin and *Compact* genetic background, we could separately study the effect of *Compact* myostatin mutation and genetic background on morphology, metabolism, and signaling.

We defined the following aims in our study:

1. To analyse the body composition of the *Compact* mice.
2. To characterize the tissue glycogen distribution and skeletal muscle cellularity in *Compact* mice.
3. To examine the metabolic effects of the *Compact* mutation.
4. To identify the molecular consequences of the *Compact* mutation which can regulate skeletal muscle and liver size, and the metabolism.

MATERIALS AND METHODS

Animals and sample collection

We performed the study on male, 3-4 and 10 months old *Compact* (*Compact* myostatin and *Compact* genetic background), congenic wild-type (wild-type myostatin and *Compact* genetic background), and BALB/c (wild-type myostatin and wild-type genetic background) mice. The *Compact* mice were crossed with BALB/c to introgress the wild-type myostatin gene of BALB/c to *Compact* mice. The wild-type myostatin allele was followed through five generations of repeated backcrossing with the *Compact* line. Heterozygous animals of this line in generation B5 were mated inter se to give homozygous wild-type animals with *Compact* genetic background (denoted as congenic wild-type animals). Animal experiments conformed to the National Institutes of Health Guide for the Care and Use of Laboratory animals (NIH Pub. No. 85-23, Revised 1996) and were approved by the local Ethics Committee at the University of Szeged. The quadriceps femoris (QF), gastrocnemius (Gastro), tibialis anterior (TA) muscles, and organs were removed. The tissue samples were frozen immediately in isopentane cooled by liquid nitrogen and stored at - 80°C until further processing.

Determination of glycogen and protein content by spectrophotometry

Muscle and liver glycogen was measured as glucose residues after acidic hydrolysis by a standard enzymatic assay. Briefly, following cryogenic milling the samples were digested at 100°C. After lysis the samples were cooled to room temperature and neutralized. Thereafter, the samples were centrifuged and the supernatants were removed. The concentration of glucose was determined from the supernatant by Hexokinase kit (Roche, Mannheim, Germany).

Muscle and liver samples were homogenized containing protease inhibitor cocktail (Sigma-Aldrich, St. Louis, MO, USA) to extract the total protein amount. The incubation of the samples was followed by centrifugation to remove cellular debris. The protein content was determined by BCA Protein Assay Reagent (Thermo Scientific, Rockford, IL, USA). Spectrophotometry was performed on Fluostar Optima (BMG Labtech, Ortenberg, Germany)

PAS-staining

Glycogen was detected by performing Periodic Acid Schiff (PAS)-staining cryosections of the TA muscle and liver samples. Sections were fixed in formaldehyde in ethanol and incubated periodic acid, followed by washing. Then the sections were incubated in Schiff's reagent, followed by incubation in potassium metabisulfite solution. Thereafter, washing of the slides tap water and deionized water. Finally, the sections were incubated in ethanol and toluol, then were mounted with Entellan.

Immunohistochemistry

Fiber-type analysis was performed cryosections of the midbelly region of TA muscle. The sections were blocked, and then incubated with mouse monoclonal primary antibodies. BA-D5, sc-71 and BFF3 primary antibodies were used, specific for Myosin Heavy Chain I (MyHCI), MyHCIIA and MyHCIIB. After incubation with the peroxidase-conjugated secondary antibody, the immunocomplexes were visualized by 3,3'-diaminobenzidine. We could not detect BA-D5 positive (MyHCI) fibers in the TA muscle; therefore, the fibers stained with neither MyHCIIA nor MyHCIIB were considered as MyHCIIX fibers.

Determination of the total fiber number and glycogen content of the whole cross sectional area

Photos were taken using a Nikon Labophot-2 microscope equipped with Olympus DP71 camera. The full cross sectional areas (CSAs) of the muscles were reconstructed from the microscopic images by Cell*B software (Olympus DP Soft software, Version 3.2., Soft Imaging System GmbH; Munster, Germany). The glycogen content of an individual fiber can be predicted by multiplying the average intensity of PAS-staining by the CSA of the fiber. Average intensity of PAS-staining (0-1 OD), CSAs of all fibers and fiber numbers were determined on the whole muscle CSA on greyscale converted PAS-stained, panoramic images by Digimizer software (Medcalc software, Mariakelke, Belgium).

Determination of the glycogen content of the different fiber types

The fiber-type specific average intensity of PAS-staining and the CSAs of the different fiber types were determined on 2-3 representative microscopic fields of both superficial and deep regions of the TA muscle. Both the sc-71 (MyHCIIA) and the BF-F3 (MyHCIIB) stained regions were matched with the PAS-stained identical regions on serial sections to analyze the glycogen content of the different fiber types.

Western blotting

The M. gastrocnemius and liver samples were homogenized supplemented with protease inhibitor cocktail (Sigma-Aldrich, St. Louis, MO, USA), natrium-orthovanadate and natrium-fluoride. The samples were separated on SDS-polyacrylamide gel, and were transferred onto Protran nitrocellulose membrane (Amersham, GE Healthcare). After incubation in blocking agent the membrane was incubated with primary antibodies, followed by incubation with appropriate horseradish peroxidase-conjugated anti-IgG secondary antibody. ECL reagent (Advansta, Menlo Park, CA, USA) was used for substrate detection, and the membrane was exposed to X-ray film for visualization.

Measurement of tissue alanine aminotransferase activity

The activity of alanine aminotransferase (ALT) enzyme of the liver samples was determined by lactate dehydrogenase coupled kinetic colorimetric assay (Diagnosticum Inc.,

Budapest, Hungary) in accordance with the manufacturer's instructions. Spectrophotometry was performed with Fluostar Optima (BMG Labtech, Ortenberg, Germany).

Intraperitoneal pyruvate, glucose, and insulin tolerance tests

For intraperitoneal pyruvate tests 3-4 months old male mice were fasted. Blood glucose after intraperitoneal pyruvate injection (2 mg pyruvate / 1 g body weight) was measured at 15, 30, 45, 60, 90, and 120 min. For intraperitoneal glucose tolerance test, 3-4 and 10 months old male mice were fasted. The blood glucose after the intraperitoneal glucose injection (2 mg glucose / 1 g body weight) was determined from distal tail vein at 30, 60, 90, and 120 min. For intraperitoneal insulin tolerance test (1.0 U / 1 kg body weight; Humulin R, Eli Lilly, B.V Grootslag, Netherlands), animals in same age. After the injection of intraperitoneal insulin bolus blood glucose was measured at 15, 30, 45, 60, 90, and 120 min.

Small-animal PET/MRI imaging using 2-deoxy-2-(^{18}F)fluoro-D-glucose

10 months old male mice were injected ^{18}FDG (2-deoxy-2-(^{18}F)fluoro-D-glucose). Whole body PET scans were acquired using the preclinical *nanoScan* PET/MRI system (Mediso Ltd., Hungary). For the determination of the anatomical localization of the organs and tissues, T1-weighted MRI scans were performed PET volumes were reconstructed using a three-dimensional Ordered Subsets Expectation Maximization (3D-OSEM) algorithm (Tera-Tomo, Mediso Ltd., Hungary). Reconstructed, reoriented and co-registered images were further analyzed with InterView™ FUSION (Mediso Ltd., Hungary) dedicated image analysis software. Radiotracer uptake was expressed in terms of standardized uptake values (SUVs). Ellipsoidal 3-dimensional Volumes of Interest (VOI) were manually drawn around the edge of the tissue or organ activity by visual inspection using InterView™ FUSION multi-modal visualization and evaluation software (Mediso Ltd., Hungary).

Statistical analysis

Statistical evaluations were performed by either one-way ANOVA and Newman-Keuls post-test or unpaired t-test (GraphPad Software Inc., USA). All data are presented as mean ± SEM.

RESULTS

Body composition of the *Compact* mice

The body weights of the congenic wild-type mice carrying the wild-type myostatin gene in *Compact* genetic background were higher than BALB/c mice, but they were smaller than the *Compact* animals. The absolute weights of individual hindlimb muscles such as tibialis anterior, gastrocnemius, or quadriceps femoris muscles were almost 2-times greater in *Compact*s compared with congenic wild-type animals, and they were bigger in congenic wild-type animals than in BALB/c mice. The muscle weight/body weight ratios showed the highest values in *Compact*s and the lowest in congenic wild-type mice.

We found that the absolute weight of heart and kidney of the *Compact* and congenic wild-type mice were comparable and higher than that of BALB/c. The absolute weight of abdominal fat increased by ~30 % in 3-4 months old and ~50 % in 10 months old congenic wild-type compared with *Compact*s mice, and it was markedly lower in BALB/c group than in *Compact*s. Liver/body weight ratio of *Compact*s was smaller than that of congenic wild-type animals in both ages. Abdominal fat/body weight ratios were comparable in *Compact* and BALB/c animals, and it was almost 2-fold higher in congenic wild-type mice.

Tissue glycogen and protein distribution

To distinguish the role of *Compact* mutation and the *Compact* genetic background in the regulation of glycogen stores here we compared the glycogen content of *Compact*, congenic wild-type and BALB/c muscles. We found that total glycogen levels of *Compact* muscles were the highest, the congenic wild-type and BALB/c samples contained comparable and smaller amount of glycogen. However, the glycogen concentration was the highest BALB/c mice and displayed no differences between *Compact* and congenic wild-type groups. Analyzing the total glycogen amount and glycogen concentration we did not observe differences between congenic wild-type and *Compact* groups; the glycogen content/liver weight ratio of BALB/c animals was more than 2.5-fold smaller. The visualization of glycogen by PAS-staining verified the results of spectrophotometry, weaker staining was observed in BALB/c samples. We determined the total protein amount in the investigated muscles and we found that the total protein content of the *Compact* muscles were the highest and the congenic wild-type and BALB/c samples contained smaller amount of protein in

accordance to total glycogen levels. Furthermore, we measured the total hepatic protein content and we found that it was the highest in *Compacts* and lowest in the congenic wild-type group.

Muscle characteristics of the *Compact* mice

We tested, whether the higher glycogen amount of the *Compact* muscle is caused by the changes in the glycogen content of the individual muscle fibers. To analyze this, first we determined the average intensity of PAS-staining and fiber sizes on the whole CSA of the TA muscle. The average intensity of PAS-staining did not show significant change in *Compact* muscle fibers compared to those of the wild type muscle, and no significant difference was observed regarding the average CSAs of the fibers either. The average intensity of PAS-staining multiplied by the value of fiber size is suitable to estimate the average glycogen content of the individual fibers. Comparing the average glycogen content of the fibers we could not detect any significant changes between the two groups of animal. The fiber number increased 1.7-fold in *Compact* animals. Multiplying the average glycogen content of the individual fibers by the increased fiber number we detected a similar, two-fold increase in the glycogen content of the whole muscle by PAS-staining as measured by spectrophotometry. Taken together, the average glycogen content of the individual fibers did not change; therefore, the increased fiber number can explain the elevated glycogen amount of the *Compact* TA muscle.

Glycogen content of the different fiber types

Regarding the fiber composition of the *Compact* muscle, we could not detect the slow MyHCI isoform in TA muscles in accordance with the literature. The ratio of IIB fibers increased 1.6-fold with concomitant decreases of IIX and IIA fibers indicating a glycolytic shift. Because the number of IIA fibers in *Compact* TA was very low, we could not perform statistical analysis on this type of fibers. Remarkable differences were observed comparing the sizes of the different fiber types on the whole CSA of the muscle. As in wild type animals, the CSA of type IIB fibers was 1.44-fold larger than those of type IIX; and IIX fibers were 1.52-fold larger than the IIA ones. In *Compact* mice we found a similar result: the CSA of type IIB fibers was 1.62-fold bigger than those of IIX fibers. Comparing the two mice lines

we did not find any differences between the average size of either IIB or IIX fibers. The frequency distributions of both the IIX and IIB fiber sizes showed similar shapes in *Compact* and wild type mice. The histograms of IIX fibers revealed right-skewed distribution in both groups of animals. In case of IIB fibers the bellshaped curves were wider in *Compact* and BALB/c animals than those of IIX fibers.

According to fiber size we found similar results, *i.e.*, the area of IIB fibers was the greatest, with no differences between the superficial and deep regions of the TA muscle in either mouse line, and no changes were observed regarding the fiber sizes of the two mice strains. To compare the effect of the *Compact* mutation on the fiber-type specific glycogen content of the muscle, we measured the average intensity of PAS-staining of the different fiber types on serial cryosections stained with antibodies against the different types of MyHC isoforms and PAS, respectively.

The average intensity of PAS-staining showed a similar decreasing tendency in a rank order IIA>IIX>IIB on the whole CSA of the muscle: IIB fibers exhibited the weakest OD, as in the superficial and deep regions in both mouse lines. The average intensity of PAS-staining of the different fiber types did not show significant differences between the *Compact* and BALB/c fibers on the whole muscle CSA, and no significant changes could be observed comparing the PAS intensity of the fiber types in the superficial and deep regions either. However, the frequency distribution revealed differences despite the similar average values of intensity of PAS-staining in *Compact* and wild type mice: the *Compact* TA muscle contained populations of IIX fibers with higher, and IIB fibers with both higher and lower intensity of PAS-staining resulting in a wider distribution in mutant animals.

Next, the average glycogen content of the different fiber types was compared in both strains. The average glycogen content of the IIB fibers was greater than those of IIX fibers, whereas the IIA was the lowest in the superficial and deep regions of wild type muscle.

The results indicated significant difference in the superficial region of BALB/c animals. The fiber type specific glycogen content on the whole CSA revealed similar tendency; however, without any significant changes. In parallel with the frequency distribution of PAS intensity, histograms of the average glycogen content showed that the *Compact* TA muscle contains a population of IIX fibers with higher, and IIB fibers with both higher and lower glycogen content.

Finally, we compared the total glycogen content of the different fiber types in the TA muscle. The glycogen index of IIB fibers was the highest, so that the IIB fibers stored the most glycogen in both BALB/c and *Compact* mice. The glycogen index value of IIX fibers was 2.7-fold larger in BALB/c mice compared to *Compact* animals in line with the higher number of IIX fibers present in BALB/c mice. In contrast the glycogen index of IIB fibers was 1.5-fold bigger in *Compact*s in good accordance with the increased proportion of IIB fibers in *Compact* mice.

Glucose tolerance and insulin sensitivity are improved by *Compact* myostatin mutation and reduced by *Compact* genetic background

Our results did not show any significant changes in fasting blood glucose levels comparing *Compact* mice with age-matched congenic wild-type and BALB/c animals; however, the response to exogenous glucose revealed differences between genotypes. *Compact* and BALB/c mice showed greater glucose tolerance compared with age-matched congenic wild-type strain. The area under the curve of blood glucose concentrations during the glucose tolerance test was significantly higher in congenic wild-type mice compared to age-matched *Compact* and BALB/c.

We performed insulin tolerance tests to measure blood glucose changes following insulin administration. Insulin treatment reduced blood glucose levels in all groups of mice, indicating the insulin responsivity. Congenic wild-type mice showed weaker insulin sensitivity compared with *Compact* and BALB/c groups. The area under the curve value during insulin tolerance test was significantly higher in congenic wild-types than in *Compact* and BALB/c mice at both ages. Both glucose tolerance and insulin sensitivity tests showed comparable results between age-matched *Compacts* and BALB/c mice. To test the effect of aging on glucose tolerance and insulin sensitivity, the area under the curve values were compared. The area under the curve values during insulin tolerance test of young animals were not significantly different from middle-aged groups, although they tended to be smaller in all three genotypes.

Compact mutation increases ^{18}FDG uptake in skeletal muscle, liver, and adipose tissue

The ^{18}FDG accumulation of the skeletal muscle was comparable in *Compact*s and BALB/c animals, and moderate uptake was observed in congenic wild-type animals. The radiotracer uptake of white adipose tissue showed similar results as skeletal muscle, mild uptake was observed in the congenic wild-type mice, and it was higher in *Compact* and BALB/c animals. The liver of *Compact* mice showed the highest SUVmean (standard uptake volume), which was followed by the congenic wild-type and BALB/c groups.

Liver characteristics in _Compact_ mice

We found that liver mass and liver/body weight ratios are not increased in proportion to skeletal muscle mass in *Compact* mice; therefore, we aimed to assess whether ALT activity in proportion to body weight is also reduced similarly to myostatin knock-out animals. Our data show that total liver ALT activity/body weight ratio was the lowest in *Compact*s and was the biggest in BALB/c mice. Next we administered glucose precursor pyruvate to measure hepatic gluconeogenesis. The intraperitoneal pyruvate tolerance test showed that hepatic gluconeogenesis increased in *Compact* and congenic wild-type animals compared to BALB/c animals.

The _Compact_ mutation of myostatin propeptide decreases myostatin formation

We were able to detect mature myostatin dimer in *Compact* skeletal muscle. Western blot analysis showed that the level of mature myostatin dimer was the lowest in *Compact* muscle and highest in BALB/c mice in accordance with the skeletal muscle weights of the animals. The anti-propeptide antibody could recognize the mutant propeptide, and the expression level of propeptide was proportional to myostatin level when the genotypes were compared; the lowest amount was detected in *Compact* samples.

Effects of _Compact_ myostatin mutation and genetic background on signaling

We could detect the mature myostatin; therefore, we investigated myostatin signaling in both skeletal muscle and liver. Despite low levels of myostatin protein in *Compact* skeletal muscle, the level of phospo-Smad2 was the highest when the genotypes were compared, suggesting the potential role of other TGF-β members in Smad2 activation. Phospho-Smad2

levels of the liver samples were the lowest in BALB/c mice and the highest in *Compact*s. The level of phospho-Smad1/5/8 was significantly higher in muscles of *Compact*s compared to congenic wild-type samples. However, we have not found any significant differences in phospho-Smad1/5/8 levels of liver samples between the genotypes. Furthermore, no differences were observed between either muscular or hepatic Smad4 levels. We determined the phosphorylation level of Akt. The phospho-Akt^{Ser473}/Akt ratio of congenic wild-type liver was lower than that of *Compact* and was comparable with BALB/c values. In contrast, phospho-Akt^{Ser473}/Akt ratios were higher in *Compact* and congenic wild-type muscles compared to BALB/c samples in accordance with myostatin levels.

AS160 (Akt substrate of 160 kDa), a Rab GTPase-activating protein can regulate the translocation of GLUT4 glucose transporter to the plasma membrane of insulin sensitive cells. The level of phospho-AS160 was lower in congenic wild-type muscle samples comparing to those of *Compact* or BALB/c mice. The GLUT4 expression showed equal levels in *Compact* and congenic wild-type animals, and the level was lower in BALB/c samples.

CONCLUSIONS

In the present thesis we investigated the effects of the *Compact* mutation *Mstn(Cmpt-dl1Abc)* on the morphology, metabolism, and signaling **(Figure 2)**.
The major findings of the thesis are as follows:

1. We have found that both the *Compact* mutant myostatin and the genetic background increases the skeletal muscle size.

2. The increased glycogen and protein content of the *Compact* muscles may lead to increased skeletal musle mass.

3. Although the average glycogen content of the individual fibers kept unchanged in *Compact* muscle, the number of IIB and IIX fibers increased leading to increased glycogen content of the muscle.

4. Both the *Compact* myostatin and the genetic background exhibit systemic, metabolic effects.

5. The *Compact* mutation does not influence the absolute weight of the internal organs (heart, kidney, liver, abdominal fat) despite the increased absolute weight of the skeletal muscle.

6. The genetic background increases the absolute weight and glycogen content of the liver; furthermore, it increases the glucose uptake and hepatic gluconeogenesis.

7. The *Compact* myostatin decreases adipositiy, improves insulin sensitivity, enhances the glucose uptake of the skeletal muscle and white adipose tissue, whereas the genetic background has opposite effects.

8. The *Compact* mutation does not prevent the formation of myostatin; however, it decreases the amount of mature myostatin leading to altered activation of Smad2, Smad1/5/8 and Akt.

9. The increased level of phospho-AS160^{Thr642} in *Compact* samples myostatin may lead to increased glucose uptake of the skeletal muscle.

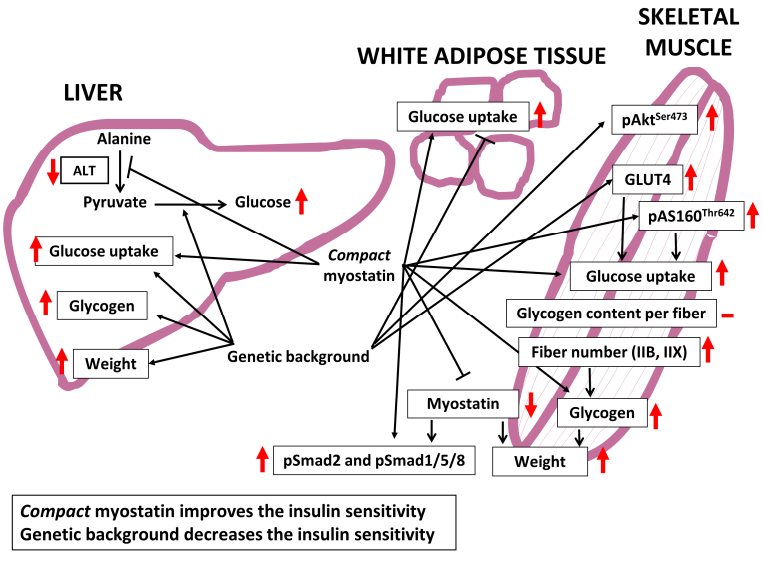

Figure 2. *The major conclusions of the thesis. The metabolic effects of the Compact myostatin and the genetic background can compensate for each other.*

ACKNOWLEDGEMENTS

These studies were supported by the European Union and the State of Hungary and cofinanced by the European Social Fund in the framework of the TÁMOP 4.2.4. A/2-11-1-2012-0001 “National Excellence Program”, GINOP-2.3.2-15-2016-00006, and GINOP-2.3.2-15-2016-00040.

Firstly, I would like to give my special thanks for Professor László Dux for providing possibility for my work and encouraged me to join the Department of Biochemistry.

I would like to give my greatly thanks for Anikó Keller-Pintér for supervising and the helpful advices for my work during on graduate as well as PhD years. She greatly introduced me to the scientific work and analytical thinking.

I would like to give my thanks for my co-authors. Especially, György Trencsényi for the PET/MRI measurement and Géza Müller for his advices in mice crossing and Ferenc Deák for his critical reading and help in the manuscript drifting.

Furthermore, I would like give my thanks to Kitti Szabó for her help during the experiments.

I would like to give my greatly thanks for Lászlóné Csontos for his excellent assistance during my experimental work and Zita Makráné Felhő and Istvánné Balásházy for their assistance and help during my PhD years.

I would like my thanks to all of my former colleagues in the Department of Biochemistry. Last but not least I would like give my greatly thanks for my family to supported me during my work.